

HINS R&D Collaboration on Electron Cloud Effects: Midyear Progress Report*

M. A. Furman[†]

Center for Beam Physics

Lawrence Berkeley National Laboratory, Bldg. 71R0259

1 Cyclotron Rd.

Berkeley, CA 94720

(Dated: 22 September 2006)

We present a status report on ongoing activities on electron-cloud R&D for the MI upgrade. These results update those presented in Ref. 1, pursuant to an MOU signed between URA Inc./FNAL and LBNL in May of 2006, and subsequently amended.

I. E-CLOUD BUILD-UP SIMULATIONS.

We have understood and fixed a bug in the POSINST code, specifically in the Poisson solver used in the computation of the electron space-charge self-forces. This bug arose intermittently, and its most serious manifestation was the appearance of virtual cathodes (regions of high electron density very close to the walls of the chamber) at high beam intensity and/or high peak SEY. These virtual cathodes were most likely due to the inadequate computation of the space-charge fields, and sometimes crashed the code. For MI simulations, the debugged code yields results only a few percent different from the old ones [1] provided the artificial virtual cathode does not materialize. On the other hand, for the case of the LHC, the debugged code yields results for the ecloud density and power deposition up to $\sim 40\%$ lower than the previous ones [2], so we conclude that this issue depends on the parameter regime in question.

We have now incorporated a new Poisson solver in POSINST, which is based on an efficient multigrid algorithm. The code is now less prone to lead to artificial virtual cathodes, although we expect these to reappear when we really push the beam intensity and/or the SEY. This expectation is based on a shortcoming of the SEY physical model that remains in the code, namely that the SEY is wholly independent of the space-charge forces. We have tested the new Poisson solver in stand-alone mode fairly extensively, so we are confident that it gives the correct (indeed, quite accurate) results.

We have also gone through the methodical and tedious exercise of varying computational parameters (time step size, space-charge grid size, and maximum number of macroparticles allowed) to make sure we understand the minimal conditions necessary for adequate numerical convergence. We felt more confident doing this exercise in the context of the LHC dipole ecloud buildup simulations because we have older results to compare this

with, in addition to the similar results carried out by the CERN group with their code ECLOUD. We believe we have identified sensible criteria required for numerical stability, so the full exercise does not need to be repeated for the MI. Specifically, the space-charge grid for the MI needs to be 32×32 cells or denser. We have found that 64×64 affords a good compromise between accuracy and CPU time, and that the average number of macroparticles needs to be not less than $\sim 5 - 10$ per grid cell when space-charge forces are important. CPU time used by POSINST with the new Poisson solver for a 64×64 grid is only $\sim 30\%$ larger than with the old solver with a 26×10 grid, and is, of course, much more accurate. Fig. 1 shows a 64×64 grid superimposed on the MI chamber cross-section.

For the MI upgrade we have run several simulations for a field-free region and for a dipole magnet, and they show a slightly smaller ecloud saturation density than before [1]. Sample results for a field-free region are shown in Figs. 2-7. The parameters used to obtain these results are the same as those listed in Ref. 1, except that now we have:

1. Used the new multigrid Poisson solver with a grid of 64×64 cells instead of the old (buggy and slow) solver with a grid of 26×10 cells.
2. Used an injection beam energy $E_b = 8.9$ GeV instead of 8 GeV.
3. Used 10 times more primary macroelectrons per bunch passage than before (input parameters `macroionel=90`, `macroplel=10` rather than `macroionel=9`, `macroplel=1`).
4. Set a limit of 20000 for the maximum number of macroelectrons allowed in the simulation at any given time instead of 2000 (input parameter `nemax`).
5. Used typically only 2 booster batches (168 bunches) instead of 6 to save on CPU time (however, all average quantities shown in Figs. 3-7 were computed in steady state, typically reached $\sim 1.5 \mu\text{s}$ after injection; this allows $\gtrsim 1.5 \mu\text{s}$ of steady state during which to compute averages).

*Work supported by the FNAL HINS R&D Effort and by the US DOE under contract DE-AC02-05CH11231.

[†]Electronic address: mafurman@lbl.gov; URL: <http://mafurman.lbl.gov>

6. Allowed the RMS bunch length σ_z to vary in $0.1 \leq \sigma_z \leq 0.75$ m in Figs. 5-7 instead of keeping it fixed at 0.75 m.

II. E-CLOUD EFFECTS ON THE BEAM.

With HINS funds we have hired postdoc Kiran Sonnad, formerly at SLAC, to work on many of these issues. Kiran came on board September 6th, 2006. Yesterday (Sept. 21) he succeeded in porting the 3D self-consistent code WARP/POSINST to his PC and carried out a very first simulation of the MI beam emittance evolution due to the ecloud (Fig. 8). Jean-Luc Vay, an LBNL staff and the main WARP/POSINST maintainer/developer, has been instrumental in transferring the code to us. He has also augmented the code with a “quasi-static mode” of operation, which is half-way between a 0th-order simulation and a full self-consistent simulation of the beam-ecloud system. In this approximation a given bunch in the beam, represented by macroprotons, interacts with an initially-uniform 2D ecloud at one (or a few) discrete locations (called “stations”) around the ring. During the passage of the bunch through the ecloud the beam particles and the electrons move in the transverse plane under their mutual influence. The ecloud at each station is refreshed before the next bunch passage. After a bunch passes through a station, it is transported to the next station by means of a lattice map (a map capability has also been recently implemented in WARP/POSINST by Jean-Luc Vay). Last week, Jean-Luc succeeded in getting preliminary results on emittance growth for the case of the LHC beam, showing good agreement with similar simulations obtained by CERN personnel with their own code “HEADTAIL.”

III. MICROWAVE PROPAGATION THROUGH THE E-CLOUD.

Kiran is also getting started on MOU item 6 (microwave transmission through an electron cloud). He’s started to read the basic papers by F. Caspers and T. Kroyer (CERN) on their experiments at the SPS [3–5].

IV. POSINST STATUS.

We’d like to transfer the debugged/improved POSINST to FNAL personnel (MOU item 7) soon, after a few more tests and improvements are carried out. But a working version is available at any time upon request.

V. NEAR-FUTURE ACTIVITIES.

1. Complete build-up simulations as described in the MOU. Pay special attention to new ecloud measurements at the MI [6] and the SEY measurements of FNAL chamber material samples at SLAC [7].
2. Continue and augment WARP/POSINST simulations to study the effects of the ecloud on the beam.
3. Gradually refine the analysis of the microwave transmission through the ecloud (eg., take into account effects of the actual chamber shape, ecloud temperature and non-uniformities, presence of the beam, etc.)

-
- [1] M. A. Furman, “A preliminary assessment of the electron cloud effect for the FNAL main injector upgrade,” LBNL-57634/CBP-Note-712/FERMILAB-PUB-05-258-AD, 23 June 2006.
- [2] M. A. Furman and V. H. Chaplin, “Update on electron-cloud power deposition for the LHC arc dipoles,” LBNL-59062/CBP Note 723, January 30, 2006; PRST-AB 9, 034403 (2006). <http://prstab.aps.org/pdf/PRSTAB/v9/i3/e034403>
- [3] T. Kroyer, F. Caspers, W. Höfle, J. M. Jiménez, J.-F. Malo, J. Tückmantel, “Unexpected Results on Microwave Waveguide Mode Transmission Measurements in the SPS Beam Pipe,” Proc. E-CLOUD04.
- [4] T. Kroyer, “Application of Waveguide Mode Diagnostics for Remote Sensing in Accelerator Beam Pipes,” Ph.D. dissertation, May 2005. Institut für Nachrichtentechnik und Hochfrequenztechnik eingereicht an der Technischen Universität Wien, Fakultät für Elektrotechnik und Informationstechnik.
- [5] T. Kroyer, F. Caspers, E. Mahner, “The CERN SPS Experiment on Microwave Transmission Through the Beam Pipe,” Proc. PAC05, paper MPPP031.
- [6] R. Zwaska, “Early slides,” PPT file, Sept. 2006.
- [7] R. Kirby, “SLAC SEY and Surface Analysis Measurements on FNAL Main Injector Ring S/S Beam Chamber Material,” Sept. 5, 2006.

DISCLAIMER

This document was prepared as an account of work sponsored by the United States Government. While this document is believed to contain correct information, neither the United States Government nor any agency thereof, nor The Regents of the University of California, nor any of their employees, makes any warranty, express or implied, or assumes any legal responsibility for the accuracy, completeness, or usefulness of any information, apparatus, product, or process disclosed, or represents that its use would not infringe privately owned rights. Reference herein to any specific commercial product, pro-

cess, or service by its trade name, trademark, manufacturer, or otherwise, does not necessarily constitute or imply its endorsement, recommendation, or favoring by the United States Government or any agency thereof, or The Regents of the University of California. The views and opinions of authors expressed herein do not necessarily

state or reflect those of the United States Government or any agency thereof, or The Regents of the University of California.

Ernest Orlando Lawrence Berkeley National Laboratory is an equal opportunity employer.

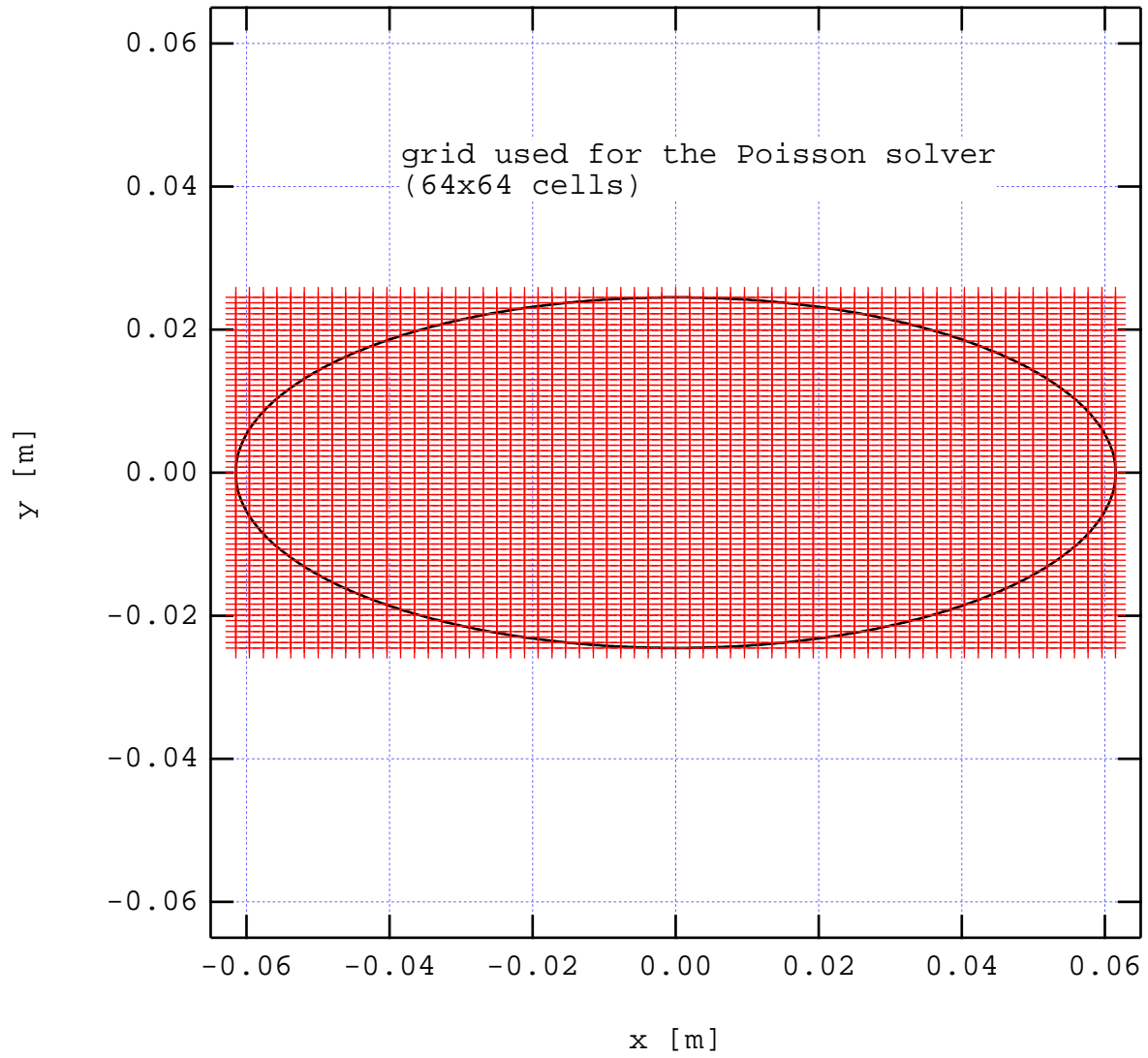


FIG. 1: MI chamber cross-section and the grid used to compute the space-charge forces. The grid is of size 64×64 cells, so that the number of cells within the elliptical chamber is $\simeq 3216$.

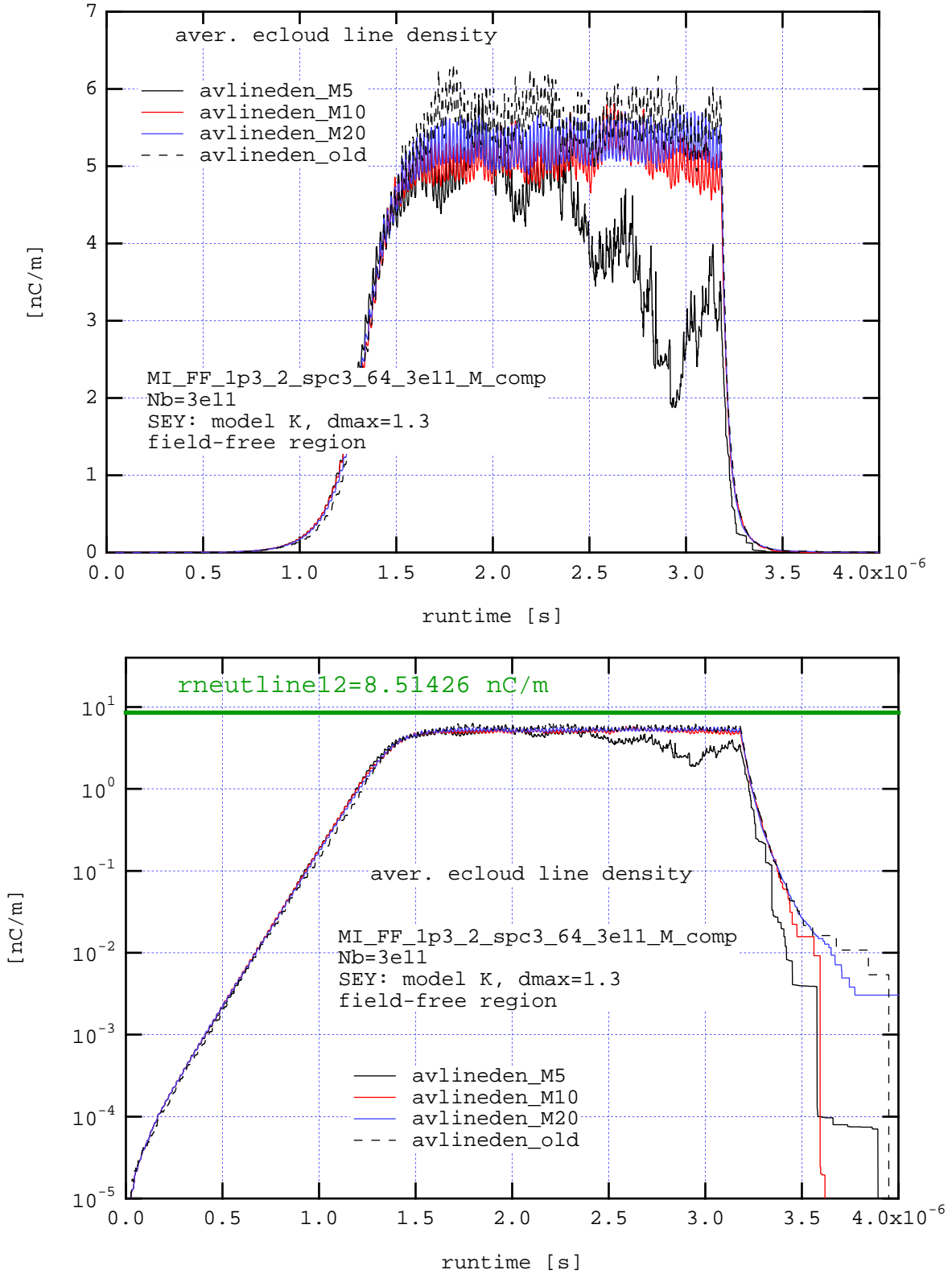


FIG. 2: Average EC line density vs. time in a field-free region for $N_b = 3 \times 10^{11}$ and $E_b = 8.9$ GeV for 2 booster batches (total 168 bunches). The SEY model used here is model “K” with $\delta_{\max} = 1.3$ [1]. The only difference between the top and bottom plots is the linear or logarithmic vertical scale. The horizontal green line represents the average beam line density, $\bar{\lambda}_b = eN_b/s_b = 8.5$ nC/m. The different traces were obtained by varying the maximum number of macroelectrons allowed (POSINST input parameter `nexmax`): the trace “M5” was obtained by setting `nexmax=5000`, the trace “M10” with `nexmax=10000`, etc. The trace “old” is the same as in Fig. 2(b) of Ref. 1, except that in the present case we used only 2 booster batches instead of 6. The deep fluctuations for the case M5 are due to the appearance of virtual cathodes, which are mostly a numerical artifact.

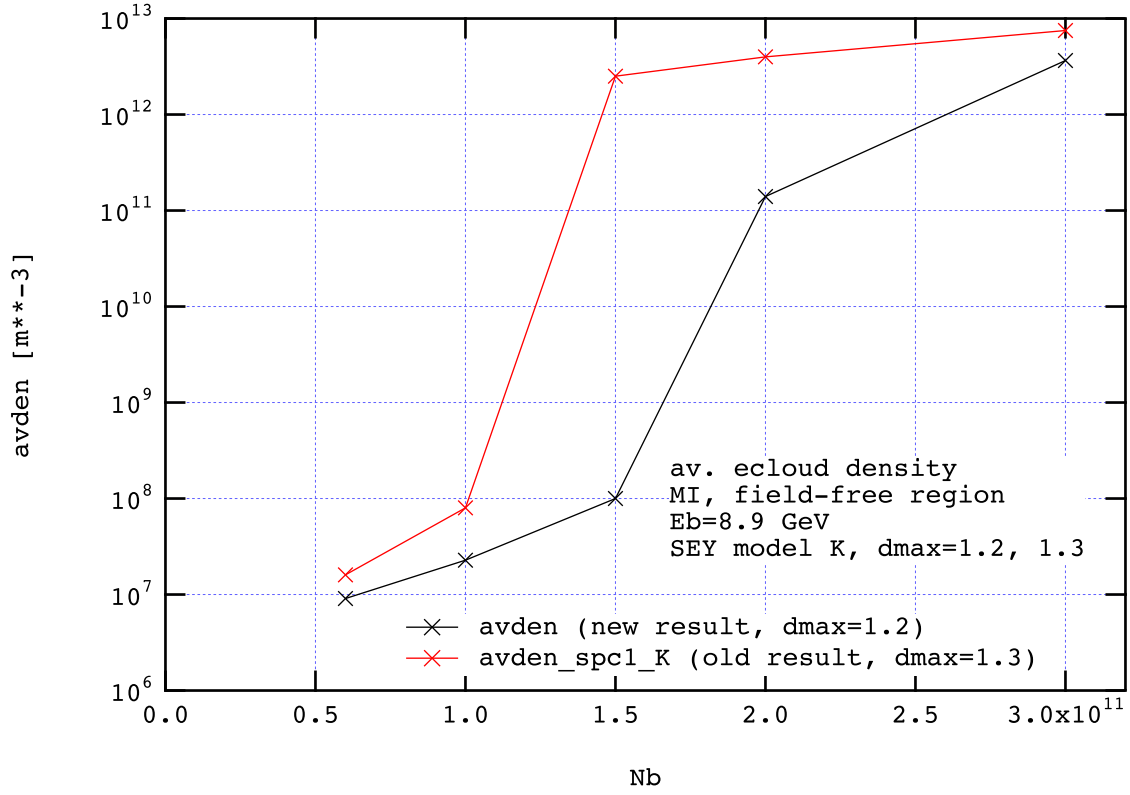


FIG. 3: Steady-state EC density near the bunch center vs. bunch intensity N_b for a field-free region, for SEY model “K” at injection beam energy. The “old” result is taken from Ref. 1, Fig. 4, and corresponds to $\delta_{\max} = 1.3$; it shows a threshold at $N_b \sim 1.25 \times 10^{11}$. The new result (black trace) was obtained for $\delta_{\max} = 1.2$, and shows a threshold at $N_b \sim 1.75 \times 10^{11}$.

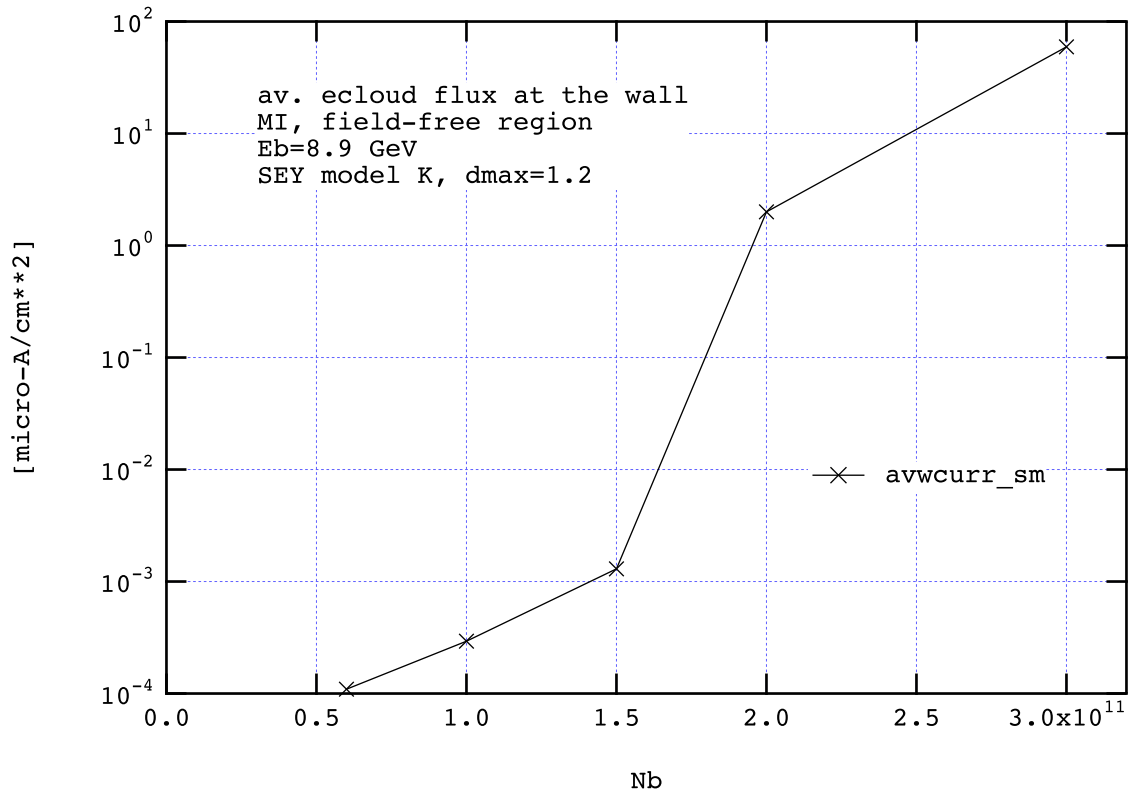


FIG. 4: Steady-state electron flux at the walls of the chamber vs. bunch intensity N_b for a field-free region at injection beam energy for SEY model “K” and $\delta_{\max} = 1.2$. For comparison, for $N_b = 3 \times 10^{11}$ and $\delta_{\max} = 1.3$, the flux is $\sim 100 \mu\text{A}/\text{cm}^2$ (Ref. 1, Fig. 3 caption).

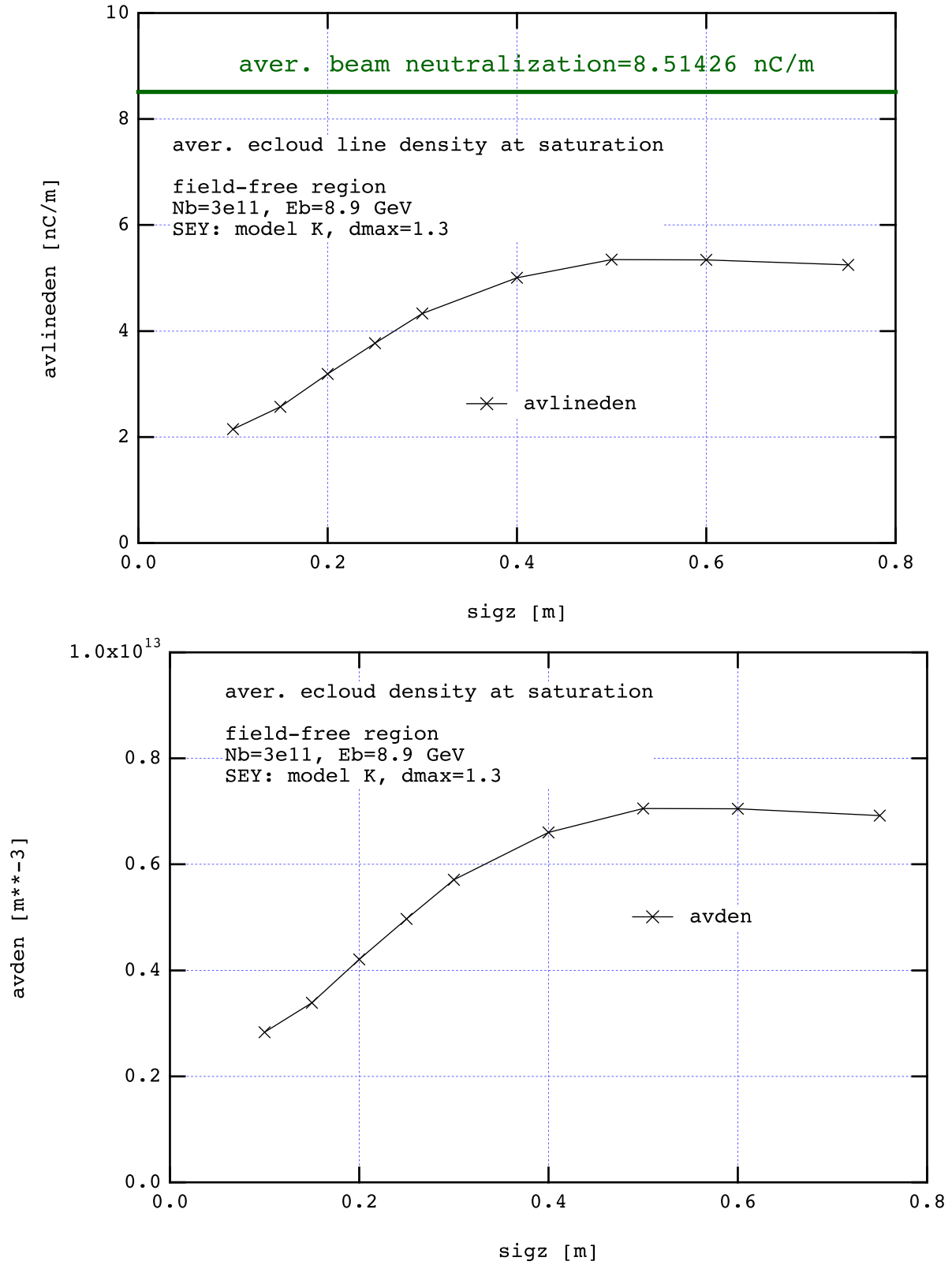


FIG. 5: Steady-state ecloud density near the bunch center vs. RMS bunch length σ_z for a field-free region, for SEY model “K” with $\delta_{\max} = 1.3$ for $N_b = 3 \times 10^{11}$ and $E_b = 8.9$ GeV. In Ref. 1, the only value used was $\sigma_z = 0.75$ m. The data in the two plots is the same, with different normalization.

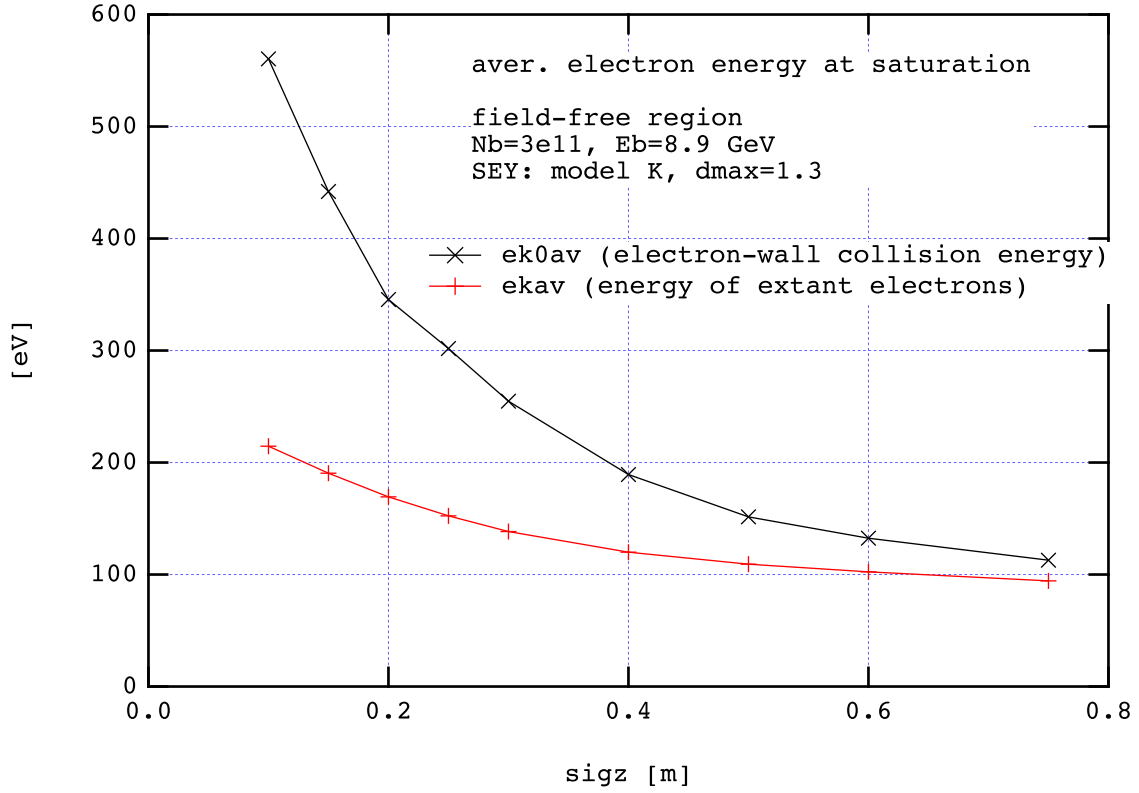


FIG. 6: Steady-state electron kinetic energy vs. RMS bunch length σ_z for a field-free region, for SEY model “K” with $\delta_{\max} = 1.3$ for $N_b = 3 \times 10^{11}$ and $E_b = 8.9$ GeV. The trace “ek0av” represents the average electron-wall collision energy, while “ekav” represents the average kinetic energy of the electrons that are “floating around” the chamber (most sensibly interpreted as the ecloud temperature). It should be remarked that the peak value of the SEY curve is reached at $E_{\max} \lesssim 300$ eV (Ref. 1 Fig. 1 and Table 1), therefore this plot implies that the effective SEY is expected to decrease when σ_z falls below ~ 0.3 m. The results shown in Figs. 5 and 7 are roughly consistent with this expectation.

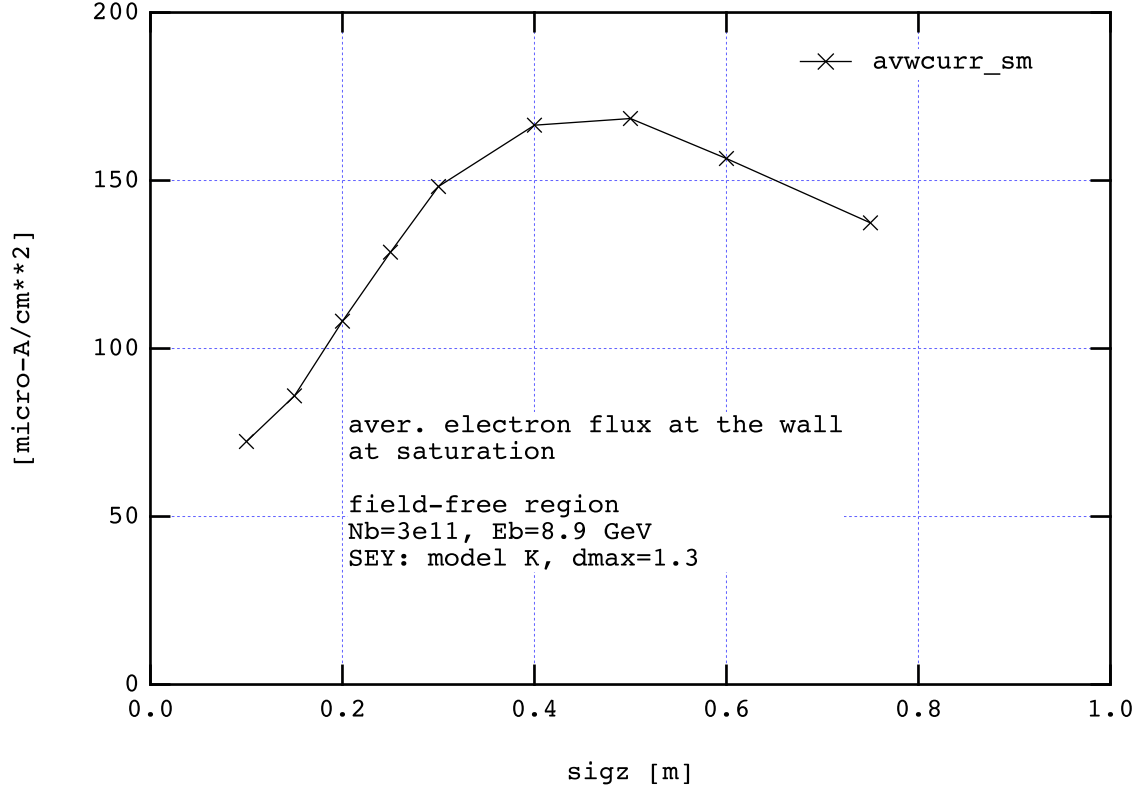


FIG. 7: Steady-state incident electron flux at the walls of the chamber vs. RMS bunch length σ_z for a field-free region, for SEY model “K” with $\delta_{\max} = 1.3$ for $N_b = 3 \times 10^{11}$ and $E_b = 8.9$ GeV. The decrease of the flux as σ_z falls below ~ 0.3 m is probably due to the effect explained in the caption of Fig. 6. The decrease of the flux as σ_z increases above ~ 0.4 m remains to be explained.

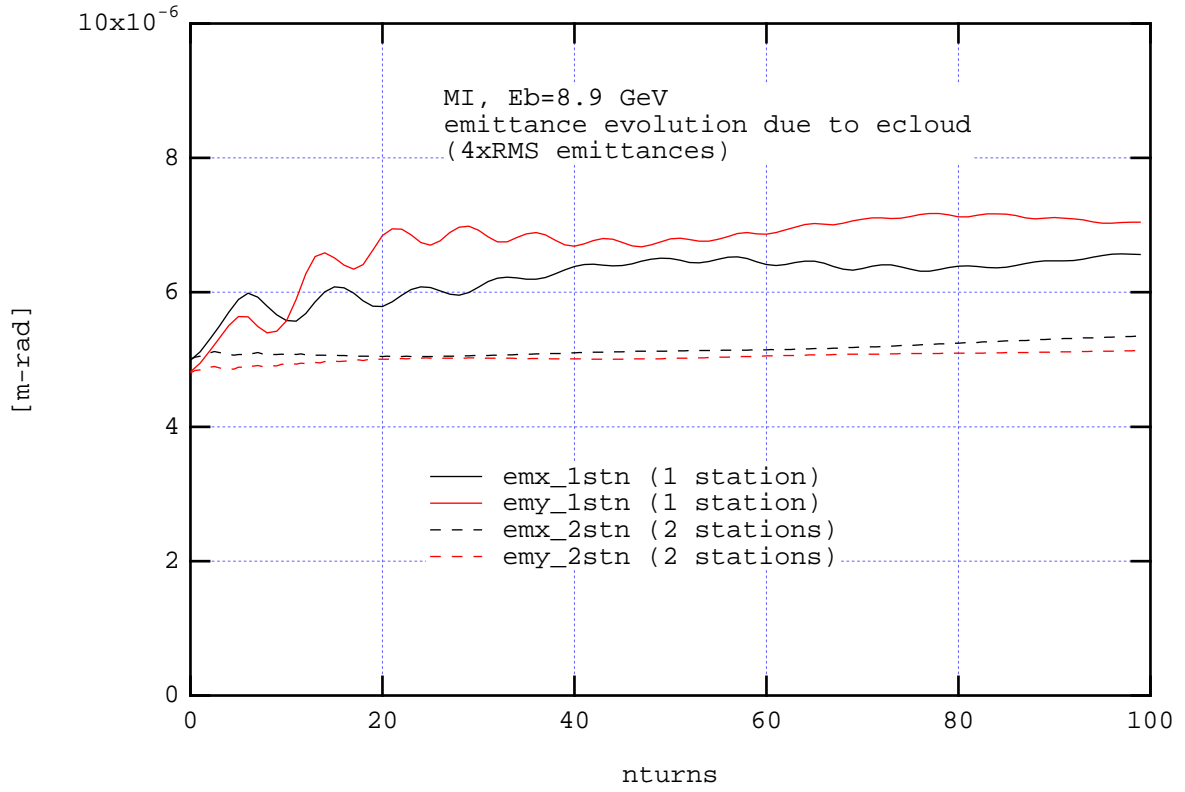


FIG. 8: A very preliminary result for the time evolution of the beam emittances due to the electron cloud obtained with the code WARP/POSINST in quasi-static mode, for $E_b = 8.9$ GeV. The two sets of traces correspond to the approximations in which the beam-ecloud interaction is lumped at either 1 or 2 points around the ring (these locations of beam-ecloud interaction are called “stations”). The lattice was assumed to be linear with tunes $(\nu_x, \nu_y) = (26.424996, 25.415003)$ and average betas $(\bar{\beta}_x, \bar{\beta}_y) = (19.9923, 20.7868)$ m. The beam was represented by 3×10^5 macroprotons, and the ecloud at each station by 1×10^5 macroelectrons.